UNICA UNIVERSITÀ DEGLI STUDI DI CAGLIARI

Off-target activity of NBOMes and NBOMe analogs at the μ opioid receptor

M.H. Deventer[1], M. Persson[2], A. Laus[3], E. Pottie[1], A. Cannaert[1], G. Tocco[4], H. Gréen[2,5], C.P. Stove[1*]

[1] Laboratory of Toxicology, Department of Bioanalysis, Faculty of Pharmaceutical Sciences, Ghent University, Ottergemsesteenweg 460, 9000 Ghent, Belgium

[2] Department of Forensic Genetic and Forensic Toxicology, National Board of Forensic Medicine, Linköping, Sweden

[3] Department of Biomedical Sciences, University of Cagliari, Italy

[4] Department of Life and Environmental Sciences, University of Cagliari, Italy

[5] Division of Clinical Chemistry and Pharmacology, Department of Biomedical and Clinical Sciences, Faculty of Medicine and Health Sciences, Linköping University, Linköping, Sweden

ORCID & e-mail adress:

Marie H. Deventer: 0000-0001-6667-2561 (marie.deventer@ugent.be)

Mattias Persson: 0000-0002-4383-2902 (mattias.persson@rmv.se)

Antonio Laus: 0000-0002-7227-513X (laus.antonio91@gmail.com)

Eline Pottie: 0000-0002-9077-4055 (eline.pottie@ugent.be)

Annelies Cannaert: 0000-0002-8654-1371 (anneliescannaert@gmail.com)

Graziella Tocco: 0000-0003-0081-5704 (toccog@unica.it)

Henrik Gréen: 0000-0002-8015-5728 (henrik.green@liu.se)

Christophe P. Stove: 0000-0001-7126-348X (christophe.stove@ugent.be)

*Corresponding author

Laboratory of Toxicology

Faculty of Pharmaceutical Sciences

Ottergemsesteenweg 460

9000 Ghent

Belgium

Tel.: +32 9 264 81 35

Fax: +32 9 264 81 83

E-mail: Christophe.Stove@UGent.be

The authors declare that they have no conflict of interest.

Abstract

New psychoactive substances (NPS) are introduced on the illicit drug market at a rapid pace. Their molecular targets are often inadequately elucidated, which contributes to the delayed characterization of their pharmacological effects. Inspired by earlier findings, this study set out to investigate the μ opioid receptor (MOR) activation potential of a large set of psychedelics, substances which typically activate the serotonin (5-HT_{2A}) receptor as their target receptor. We observed that some substances carrying the N-benzyl phenethylamine (NBOMe) structure activated MOR, as confirmed by both the NanoBiT® βarr2 recruitment assay and the G protein-based AequoScreen® Ca^{2+} release assay. The use of two orthogonal systems proved beneficial as some aspecific, receptor independent effects were found for various analogs when using the Ca^{2+} release assay. The specific 'off-target' effects at MOR could be blocked by the opioid antagonist naloxone, suggesting that these NBOMes occupy the same common opioid binding pocket as conventional opioids. This was corroborated by molecular docking, which revealed the plausibility of multiple interactions of 25I-NBOMe with MOR, similar to those observed for opioids. Additionally, structure-activity relationship findings seen in vitro were rationalized in silico for two 25I-NBOMe isomers. Overall, as MOR activity of these psychedelics was only noticed at high concentrations, we consider it unlikely that for the tested compounds there will be a relevant opioid toxicity in vivo at physiologically relevant concentrations. However, small modifications to the original NBOMe structure may result in a panel of more efficacious and potent MOR agonists, potentially exhibiting a dual MOR/5-HT_{2A} activation potential.

Key words

bioassay, μ opioid receptor, NBOMe, off-target, psychedelics, molecular docking

1. Introduction

Serotonergic psychedelics or classic hallucinogens are described to elicit alterations in perception, mood and thought, without inducing delirium, addiction or memory impairment, while having activation of the serotonin 2A receptor (5-HT_{2A}R) as their main pharmacological mechanism(Glennon et al. 1984; Nichols 2004, 2016). Aside from typically described substances such as mescaline, psilocybin, and LSD (lysergic acid diethylamide), a wide variety of psychedelic new psychoactive substances (NPS) has emerged throughout the years(Johnson et al. 2019; United Nations Office on Drugs and Crime 2020, 2021). Of specific importance in the context of NPS are the NBOMes (N-benzyl phenethylamines), with the relevance and dangers of 25I-NBOMe already being emphasized in 2014 in an EMCDDA (European Monitoring Centre for Drugs and Drug Addiction) Risk Assessment Report(European Monitoring Centre for Drugs and Drug Addiction 2014). Users of psychedelics typically seek for mystical experiences, altered consciousness, and empathic feelings, inter alia. Compared to 'typical' psychedelics, however, NBOMes have been associated with particularly severe adverse events, such as seizures, hyperthermia, and rhabdomyolysis, and fatalities have been described(Kyriakou et al. 2015; Luethi and Liechti 2020; Poulie et al. 2020). So far, the mechanism behind this particular toxicity is not fully understood(Poulie et al. 2020). Off-target modulation of other (non-5-HT_{2A}) receptors is amongst several possibilities. Apart from their 5-HT_{2A}R activation, psychedelics in general typically interact with a multitude of receptors, including both members of the 5-HT receptor family and of more distinct monoaminergic receptors. This polypharmacology is believed to contribute to the observed effects(Keiser et al. 2009; Nichols 2016). For instance, Rickli et al. reported on the binding affinity and receptor activation potential of a series of phenethylamines, including a set of NBOMes, at 5-HT_{1A}, 5-HT_{2A}, 5-HT_{2B} and 5-HT_{2C} receptor, as well as their affinity at the adrenergic α_{1A} and α_{2A} receptors, dopaminergic D_1, D_2 and D_3 receptors and the histaminergic H_1 receptor(Rickli et al. 2015).

An intrinsic connection between psychedelics and opioids has been established before. In 1986, co-administration of naloxone and DMT was found to enhance the behavioural effects of DMT in mice, while small doses of morphine and methadone seemed to antagonize the effects exerted by LSD and DMT(Domino 1986). Additionally, Marek showed the involvement of the μ opioid receptor (MOR), the main target of opioids associated with their analgesic effects, in the suppression of DOI-induced head twitches in rats(Marek 2003). Furthermore, it has been demonstrated that some opioid drugs (opioid agonists) are associated with the occurrence of serotonin syndrome, a potentially severe toxidrome caused by increased serotonergic activity in the central nervous system(Scotton et al. 2019).

The binding and activation potential of psychedelics at MOR however is described less extensively. In this context, Åstrand and colleagues recently found that certain psychedelics were able to interact with the MOR, with some compounds having a more outspoken activation potential than others(Åstrand et al. 2020). In earlier literature, Nichols et al. reported on 25I-NBOMe having significant affinity at MOR, based on the NIMH-based Psychoactive Drug Screening Program (PDSP) database (Nichols et al. 2008). Similarly, its hydroxylated counterpart 25I-NBOH showed affinity for MOR(Ettrup et al. 2011). Last, Jensen et al. described the promiscuous behaviour of another analog, 25CN-NBOH, a highly potent 5-HT_{2A} agonist(Jensen et al. 2017). The authors compiled radioligand binding assay data and demonstrated that 25CN-NBOH was capable of binding a wide array of receptors, such as serotonin, dopamine, norepinephrine, GABA, acetylcholine, as well as opioid receptors including MOR.

The NPS market is constantly evolving, with new substances being introduced to the public at a rapid pace(European Monitoring Centre for Drugs and Drug Addiction 2022). A consistent phenomenon here is the appearance of new compounds with slight structural modifications, often as a response to the scheduling of their main ‘parent’ compound(United Nations Office on Drugs and Crime 2022). This can potentially lead to the synthesis of substances with new or more pronounced characteristics. Here, we looked more into depth at the potential ‘off-target’ activity of (new) psychedelics at MOR, which is of interest as it may aid in the discovery of compounds with an unexpected pharmacological profile.

Importantly, (future) small changes in the chemical structure may potentially lead to substances with a more outspoken MOR activity or even a dual 5-HT_{2A}/MOR activity, which is relevant information for both the clinical and toxicological field. To investigate this, a panel of structurally divergent psychedelics was screened, and based on these results, we focused onto the NBOMe class of compounds. For this we applied two distinct cell-based assays, assessing either recruitment of β-arrestin 2 (βarr2), or G protein-mediated intracellular calcium release. Although MOR binding and MOR activation of a handful of NBOMe analogs has been reported, this study is the first to look specifically at the structure-activity relationship (SAR) at MOR of a large set of NBOMes. Additionally, to further investigate and better understand MOR binding by the N-benzyl phenethylamines, antagonist experiments and molecular docking were performed.

2. Materials and Methods

2.1. Materials and Reagents

Dulbecco's Modified Eagle's Medium (GlutaMAX™) (DMEM), Opti-MEM I Reduced Serum, penicillin, streptomycin and amphotericin B were obtained from Thermo Fisher Scientific (Pittsburgh, Pennsylvania, US). Dulbecco's Modified Eagle Medium: Nutrient Mixture F-12 (DMEM/Ham's F-12), HEPES buffer, trypsin, geneticin and L-glutamine were procured from Thermo Fisher Scientific (Gothenburg, Sweden) and zeocin was purchased from Invitrogen (Carlsbad, California, US). The Nano-Glo® Live Cell reagent and LCS Dilution Buffer were acquired from Promega (Madison, Wisconsin, USA). Coelenterazine was supplied by Nanolight Tech (Pinetop, Arizona, USA). Sigma-Aldrich (Stockholm, Sweden) supplied digitonin, protease-free bovine serum albumin (BSA) and adenosine triphosphate (ATP). Fetal bovine serum (FBS) and poly-D-lysine were purchased from Sigma-Aldrich (Darmstadt, Germany). The reference standard hydromorphone was obtained from Fagron (Nazareth, Belgium). JWH-018 and naloxone were procured from LGC (Wesel, Germany) (NanoBiT® assays). JWH-018 used for the AequoScreen® assays was purchased from THC Pharm (Frankfurt am Main, Germany). For preparation of the stock solutions, methanol was supplied by Chem-Lab NV (Zedelgem, Belgium), acetonitrile was bought from Biosolve (Valkenswaard, The Netherlands) and dimethylsulfoxide (DMSO) was from Sigma-Aldrich (Darmstadt, Germany). 25P-NBOMe hydrochloride, 25iP-NBOMe hydrochloride, 25G-NBOMe hydrochloride, 25T-NBOMe hydrochloride, 25T2-NBOMe hydrochloride, 25T4-NBOMe hydrochloride, 25T7-NBOMe hydrochloride, 25E-NBOH hydrochloride, 25I-NBOMe (3 MeO-isomer) hydrochloride, 25I-NBOMe (4-MeO isomer) hydrochloride, 25I-NBOMe (imine analog), N-acetyl 25I-NBOMe, 25N-NBOMe hydrochloride, 5-(2-aminopropyl)indole (5-IT), 1-(3-trifluoromethylphenyl)piperazine hydrochloride (TFMMP) and 5-methoxy-diethyltryptamine (5-MeO-DET) were kindly provided by Cayman Chemical (Ann Arbor, Michigan, US). 25I-NBMD hydrochloride, 25I-NBF hydrochloride and 25B-NBF hydrochloride were purchased from Cayman Chemical. Lysergic acid diethylamide (LSD), 2C-D hydrochloride, 2C-E hydrochloride, 2C-H hydrochloride, 2C-B-FLY hydrochloride, 25H-NBOMe hydrochloride, 25C-NBOH hydrochloride and βK-2C-B were acquired from

Chiron AS (Trondheim, Norway). DiPT hydrochloride, DMT hydrochloride, DPT hydrochloride, Bromo-DragonFLY hydrochloride, 25I-NBOMe hydrochloride, 25B-NBOMe hydrochloride, 25D-NBOMe hydrochloride, 25C-NBOMe hydrochloride, 25E-NBOMe hydrochloride, 25I-NBOH hydrochloride and 25B-NBOH hydrochloride were kindly provided by Chiron AS. 2C-I, 2C-B, 2C-C and 5-MeO-DALT were kindly gifted by Prof. K. Maudens and Prof. A. Van Nuijs (University of Antwerp), who procured 2C-B and 2C-C from Cayman Chemical, 2C-I from the Australian Government National Measurement Institute (West Lindfield, Australia) and 5-MeO-DALT from LGC Standards (Teddington, UK).

2.2. Cell culture

Human embryonic kidney (HEK) 293T cells stably expressing either the human MOR-LgBiT/SmBiT-βarr2/GRK or human cannabinoid receptor 1 (CB_1)-LgBiT/SmBiT-βarr2 system were routinely maintained at 37 °C and 5% CO_2 under a humidified atmosphere in DMEM (GlutaMAX™), supplemented with 10 % heat-inactivated FBS, 100 IU/mL penicillin, 100 mg/L streptomycin and 0.25 mg/L amphotericin B. The development of the used stable cell lines has been described elsewhere(Cannaert et al. 2016, 2017, 2018a, b; Vasudevan et al. 2020).

Calcium sensitive AequoZen recombinant Chinese hamster ovary (CHO) K1 cells, stably expressing either human MOR or CB_1, the apo-aequorin and the $G\alpha_{16}$ protein were procured from Perkin Elmer (Groningen, The Netherlands). Cells were maintained at 37 °C and 5% CO_2 under a humidified atmosphere in Ham's F12 medium supplemented with 10 % FBS, 0.4 mg/mL geneticin and 0.25 mg/mL zeocin.

2.3. In Vitro NanoBiT® MOR β-Arrestin2 recruitment assay

2.3.1. Screening for MOR activity of a panel of psychedelics

The MOR activation potential of a diverse panel of psychedelics was investigated by applying a receptor-based assay, monitoring the recruitment of the messenger protein β-arrestin2 (βarr2) to the receptor using the NanoBiT® assay principle. This is based on the functional complementation of a split nanoluciferase enzyme, which allows the detection of protein-protein interactions in living cells(Dixon

et al. 2016). In this case, one inactive subunit (LgBiT) of the enzyme is fused to the GPCR of interest (MOR), whereas the other subunit (SmBiT) is linked to βarr2 that is recruited to the receptor upon activation by an agonist (Cannaert et al. 2016, 2018b). This causes the two subunits to come into close proximity, resulting in restoration of the luciferase enzyme activity. Furimazine, the enzyme's substrate, is then converted to furimamide, yielding a bioluminescence that can be monitored using a standard luminometer.

The day prior to the assay, HEK293T cells stably expressing the MOR-βarr2 reporter system were seeded in poly-D-lysine coated, white opaque-walled 96-well plates (Greiner Bio-One, Vilvoorde, Belgium) at 50,000 cells/well and incubated overnight. All NanoBiT® experiments were carried out using cells until passage 15. The next day, cells were first rinsed twice with Opti-MEM I Reduced Serum medium, after which 100 µL was added to each well. The Nano-Glo® Live Cell reagent, which contains the cell-permeable furimazine, was diluted 20-fold in Nano-Glo® LCS Dilution Buffer and 25 µL of this substrate mix was directly added into the wells. The plate was placed into a TriStar² LB 942 Multimode Reader luminometer (Berthold Technologies, Bad Wildbad, Germany) and luminescence was monitored during an initial equilibration phase of approximately 10 minutes. Upon stabilization of the signal, 10 µL of a 13.5x concentrated test compound solution was added to the wells and luminescence was recorded for 2 hours. Stock solutions were prepared and used within 24 hours and all compounds were run in duplicate at an in well concentration of 25 µM. Hydromorphone (25 µM) was taken along and served as a positive control. Appropriate solvent controls were included on each plate.

2.3.2. Characterization of NBOMes and NBOMe analogs at MOR

The MOR-βarr2 assay was used for a further in-depth assessment of the MOR activation potential of a series of NBOMes and NBOMe analogs. Compound concentration ranges (micromolar to sub nanomolar range, similar to those earlier applied in MOR and 5-HT $_{2A}$ NanoBiT® assays) were run in duplicate in at least 3 independent experiments. Hydromorphone was taken along as a reference standard to normalize the generated data and appropriate solvent controls were present on each

plate. This assay was also used to verify the binding site of NBOMe analogs in MOR. For this, after equilibration and addition of the substrate, MOR-βarr2 cells were pretreated with 1 µM of naloxone or solvent control and left to incubate for 10 minutes prior to the addition of 2 high concentrations of test solutions to the wells. Luminescence was recorded for 2 hours.

To check for nonspecific, MOR-independent effects, a CB_1-βarr2 assay was used to screen the NBOMe analog panel at a concentration of 25 µM (in well). JWH-018 and hydromorphone (both at 25 µM) served as positive and negative controls, respectively, and all appropriate solvent controls were included. The applied protocol was the same as for the MOR-βarr2 assays.

2.4. In Vitro AequoScreen® intracellular calcium release assay

MOR activation was additionally explored using an intracellular calcium release assay, which is a considered a proxy for G protein-based signaling. For the AequoScreen® assays, cells stably expressing MOR, apoaquorin and the $G\alpha_{16}$ protein were used, allowing for the monitoring of G protein-mediated intracellular Ca^{2+} release(Stables et al. 1997). The assay principle is based on the aequorin photoprotein, found in the Aequorea Victoria jellyfish. In presence of its substrate coelenterazine, the enzyme (apoaequorin) is converted to its active form (aequorin), which can then bind Ca^{2+} ions and go through conformational changes. This results in oxidation of the coelenterazine substrate, followed by the emission of blue light and production of CO_2(Shimomura et al. 1974; Vysotski and Lee 2004; Deng et al. 2005; Bakayan et al. 2017). In the AequoZen cell system, MOR couples to and activates the $G\alpha_{16}$ protein subunit, stably expressed in this cell line, which in turn activates the phospholipase C enzyme(Connor and Christie 1999), resulting in the production of inositol trisphosphate (IP_3)(Niedernberg et al. 2003). IP_3 will then induce the rapid release of intracellularly stored calcium ions(Charlton and Vauquelin 2010), which can then bind the three Ca^{2+} sites, leading to the activation of the biosensor(Shimomura et al. 1974; Vysotski and Lee 2004; Deng et al. 2005; Bakayan et al. 2017).

AequoZen cells were cultured to a confluency of approximately 70% and harvested on the day of the assay. All AequoScreen® experiments were performed using AequoZen cells in passage 12-15. After

trypsinization for 10 min at 37 °C, the cells were centrifuged (5 min, at 1500 rpm), resuspended for counting and then diluted to 300,000 cells/mL in DMEM/HAM's F-12 medium without phenol red, supplemented with 15 mM HEPES, 2.5 mM L-glutamine and 0.1% protease-free BSA (further referred to as assay medium). Coelenterazine was added to a final concentration of 2.5 µM and the cell suspension was incubated for 3 h (room temperature, rotating, protected from light). In the meantime, agonist dilutions were prepared by serial dilution in assay medium and added to white, opaque-walled 96-well plates (Perkin Elmer). NBOMe analog concentrations ranges, similar to those analyzed using the NanoBiT® system, were tested in duplicate, run in 3 independent experiments. Digitonin (100 µM) and ATP (10 µM), both involved in the receptor-independent release of Ca^{2+} ions, served as positive controls for coelenterazine loading. Fentanyl (60 µM) was included as a positive control for MOR activation and assay medium was used as a negative control. Hydromorphone was taken along as a reference standard to normalize the generated data. After incubation, 50 µL of the cell suspension was injected into each well (approx. 15,000 cells/well) of the 96-well plate at reading cycle #10, followed by an immediate luminescence read-out (25 s, 200 consecutive measurements) using a TECAN Spark 10 plate reader (Männedorf, Switzerland).

Non-MOR-mediated effects were evaluated using the stable CB_1 AequoScreen® cell line. NBOMe analogs were tested at 3 high concentrations (corresponding to the 3 highest concentrations from the concentration range tested at MOR) and JWH-018 (60 µM) was used as a positive control for CB_1 activation. All test concentrations were tested in duplicate in 2 independent experiments. Also here, digitonin (100 µM) and ATP (10 µM) were included as positive controls and assay medium was used as a negative control. The assay was performed as described above.

2.5. Data analysis

Raw data were initially processed using Microsoft Excel 2019, after which curve fitting and statistical analysis was performed using GraphPad Prism software (Version 9.3.0) (San Diego, CA, USA).

For the NanoBiT® assay, data were base-line corrected for inter-well variability using data from the equilibration period. To generate concentration-response curves, the area under the curve (AUC) was calculated for each compound and a blank correction was performed by subtracting AUC values of the solvent controls.

For the AequoScreen® assay, AUC values were calculated based on the luminescence values recorded during measuring from cycle 10 through 200 (injection of cells at cycle #10). Values were then base-line corrected by means of linear regression using the digitonin signals, which allowed to correct for the potential drift in signal, caused by some degree of sedimentation of the cell suspension in the injector. Blank correction was performed by subtracting the AUC values of the solvent controls and data were then normalized to the maximal signal of hydromorphone (efficacy arbitrarily set at 100 %).

For both assays, the pharmacological parameters EC_{50} (a measure of potency) and E_{max} (a measure of relative efficacy) were determined by curve-fitting of the concentration-response curves via a nonlinear regression model (three parametric fit). The E_{max} of hydromorphone, which was used as a reference standard, was set at 100%, in line with earlier work(Vasudevan et al. 2020; Vandeputte et al. 2020, 2022b). The Grubbs test was used to detect outliers in the datasets, which were then omitted (p value < 0.05; applicable for 6 out of 740 (0.81 %) and 4 out of 620 (0.65 %) data points for the NanoBiT® and Aequoscreen® assays, respectively).

2.6. In silico evaluation of the 25I-NBOMe – MOR interaction

The construction of the simulated system was prepared as follows(De Luca et al. 2022). The crystal structure of the active form of (Mus musculus) MOR bound to the MOR agonist BU 72 (PDB ID, 5C1M) was obtained from the RCSB database at 2.07Å (5C1M). The protein preparation wizard tool (Maestro molecular modeling suite)(Manglik et al. 2012; Madhavi Sastry et al. 2013; Huang et al. 2015) was used to prepare and refine the structure. The Schrödinger Release 2021- 1 (Schrödinger Release 2021-1: Maestro, Schrödinger, LLC, New York, NY) with the OPLS4 force field was used to prepare and dock 25I-NBOMe, 25I-NBOMe (3-MeO isomer) and 25I-NBOMe (4-MeO isomer) into the receptor. Then, all

3 compounds were docked into the MOR binding site before equilibration and the LigPrep module was used to build all compounds at pH 7.4. Each compound was assigned a net positive charge by Epik module before preparing the MOR model using the Extended Sampling Induced Fit Docking (IFD) protocol in the Schrödinger suite. A docking grid box was located within 5 Å of the ligand and docking experiments were then performed using standard protocols. Hereby, ligand conformations were screened for clashes with proteins in the presence of an implicit membrane and solvent, and then refined by allowing side-chain flexibility upon binding(Sherman et al. 2006; Greenwood et al. 2010; Harder et al. 2016). Molecular mechanics with generalized born and surface area solvation (MM-GBSA) with default parameters and implicit membrane and solvent (Schrodinger Suite, Prime module) was used to calculate the free-binding energy of all complexes and to select the best poses.

3. **Results**

3.1. Screening of psychedelics for MOR activity

Inspired by recent work published by Åstrand et al.(Åstrand et al. 2020), reporting on the MOR activation potential of some phenethylamines, piperazines and tryptamines, a varied panel of 23 psychedelics was selected to be screened for MOR activation using the MOR-βarr2 bioassay. At a tested concentration of 25 µM, five substances activated MOR: the phenethylamine derivatives 25I-, 25B-, 25C-, 25E- and 25D-NBOMe (**Table 1**). Activity profiles of all other tested compounds overlapped with those of the solvent controls, indicating an absence of MOR activation potential at the high concentration tested. Interestingly, while for 8 compounds included in our panel Åstrand et al.(Åstrand et al. 2020) scored (some) MOR activation (indicated in bold in **Table 1**), only two of these (25I- and 25E-NBOMe) tested positive in the MOR-βarr2 bioassay.

Based on these results, an expanded set of 19 NBOMes and NBOMe analogs was screened at 25 µM, of which 5 additional substances showed opioid activity: the 4-methoxy positional isomer of 25I-NBOMe, the isopropyl analog 25iP-NBOMe, as well as the NBOH analogs 25I-, 25B- and 25E-NBOH (**Table 2**). The general N-benzyl phenethylamine structure, present in NBOMes and NBOMe analogs is depicted in **Figure 1**. An overview of the signaling profiles of all screened substances, as well as their complete chemical structures, can be found in **Supplementary Material** (**S1** and **S2**).

3.2. Pharmacological characterization

Two different cell-based assays, monitoring distinct cellular events, were used to further characterize the MOR activation potential (potency and efficacy) of the 10 compounds that scored positive during the initial screenings. Whereas the MOR-βarr2 assay assesses the recruitment of βarr2 to the activated receptor, the AequoScreen® assay allows to monitor the G protein-mediated release of calcium. **Table 3** provides an overview of the EC_{50} and E_{max} values derived from both assays. **Figure 2** displays the corresponding concentration-response curves.

Hydromorphone activated MOR as expected(Vasudevan et al. 2020; Vandeputte et al. 2020, 2022b) and showed an EC_{50} of 34.5 nM in the MOR-βarr2 assay, and an EC_{50} of 15.5 nM in the AequoScreen® Ca^{2+} assay. This substance was selected as the reference compound for normalization of the obtained data, as it has served historically as the main reference in the NanoBiT® MOR-βarr2 assay and allows comparison to earlier obtained activity data for other opioids. This enables us to critically assess the (relevance of the) MOR activation potential of the analyzed NBOMes. For consistency, the same reference was used to normalize the AequoScreen® data. Overall, both assays displayed the same rank order in potencies, although lower EC_{50} values (or higher potencies) were obtained using the AequoScreen® assay. Using the NanoBiT® assay, all compounds were found to be partial agonists relative to hydromorphone, with a rather limited MOR activation potential. Relevant in this context is the fact that hydromorphone itself is considered a partial agonist in comparison to other opioids such as fentanyl(Vandeputte et al. 2020). This implies that, in theory, normalizing the obtained NBOMe data to the E_{max} of a more efficacious compound (like fentanyl) would result in even lower NBOMe efficacies. Using hydromorphone as a reference allows us to distinguish slight differences in activation potential of weakly active compounds, such as the NBOMes, which is relevant to determine potential SAR trends. In contrast, in the AequoScreen® assay, efficacies were consistently higher than those observed with the MOR-βarr2 assay, with certain substances being scored as full MOR agonists. Of note is the 'ceiling' effect observed in the AequoScreen® assay, which complicates comparison and interpretation of the obtained efficacy values (vide infra).

In both assays, 25I-NBOMe was the most potent psychedelic, with potencies of 2.74 µM (NanoBiT®) and 876 nM (AequoScreen®) and efficacies of 22.9 % (NanoBiT®) and 97.0 % (AequoScreen®). The halogen-bearing analogs 25B-NBOMe and 25C-NBOMe were less potent, with EC_{50} values of 4.73 and 10.0 µM and efficacies of 93.6 % and 81.6%, respectively (AequoScreen®). For these compounds, calculation of EC_{50} values based on the NanoBiT® data was not possible, as a plateau of maximal activation was not reached at a concentration of 75 µM (maximal activation of 8% for 25B-NBOMe) and 100 µM (maximal activation of <5% for 25C-NBOMe). Likewise, although 25I-NBOMe (4-MeO

isomer), 25iP-NBOMe, 25E-NBOMe and 25D-NBOMe did activate MOR in both assays, accurate EC_{50} values could not be calculated because of the same reason. Estimated potencies and efficacies are presented in **Table 3**. Interestingly, based on the generated concentration-response curves, the isopropyl analog 25iP-NBOMe exhibited the most pronounced MOR activation potential in the AequoScreen® assay, reaching an efficacy of 128 % at 100 µM. This was in contrast with the MOR-βarr2 assay, in which this analog only showed 6 % MOR activity at this high concentration. Also the positional isomer 25I-NBOMe (4-methoxy) and the methyl substituted 25D-NBOMe only weakly activated MOR in the MOR-βarr2 assay (maximal activation of 7 and <5% respectively, at 100 µM). In the AequoScreen® assay these compounds also behaved as partial agonists, although yielding much higher efficacies (84 and 72 %, respectively, at 100 µM). Despite not reaching a maximum yet, the ethylated 25E-NBOMe could be considered a full agonist in the AequoScreen® assay (maximal activation of 103 % at 100 µM). Also in the MOR-βarr2 assay, this was one of the most active compounds, yielding a MOR activation of 20 % at 100 µM.

25I-NBOH was scored as a partial agonist in both assays. Using the MOR-βarr2 assay, an EC_{50} of 23.4 µM and an E_{max} of 15.8 % was calculated, and a potency of 1.33 µM and efficacy of 54.6 % was found in the AequoScreen® assay. Also 25B-NBOH and 25E-NBOH were partial agonists in the AequoScreen® assay, with efficacies of 57.0 % and 58.4 %, respectively, and respective potencies of 5.96 and 3.78 µM. For both compounds, no maximum was reached using the MOR-βarr2 assay (<5 % activation for 25B-NBOH and 19 % activation for 25E-NBOH at 100 µM) and only estimated EC_{50} values could be reported.

3.3. Determination of non-specific effects

As MOR activation by these psychedelics is considered an off-target effect, we also verified whether other (non-MOR-mediated) effects were elicited by these compounds. This is particularly relevant for the Aequoscreen® assay, as in principle activation of another receptor or pathway by the tested compounds could also yield a Ca^{2+} release (as was readily suspected for some of the compounds listed in **Table 1**)(Åstrand et al. 2020). Using the CB1-βarr2 assay, none of the compounds generated a

reproducible signal. In the AequoScreen® CB_1 assay, however, some positivity was observed for several analogs, with 25iP-NBOMe consistently showing the most pronounced signals, with a concentration of 100 µM yielding a signal comparable to that of 60 µM JWH-018. Data showing raw luminescence signals are included in **Supplementary Material S3**.

3.4. Orthosteric binding

To determine whether NBOMes and analogs bind to the MOR orthosteric binding site, their MOR activation potential was tested after blocking the receptor with 1 µM of an opioid antagonist, naloxone. Pre-treatment with naloxone antagonized MOR activation of all evaluated substances. Naloxone antagonism of MOR activation by 25I-NBOMe (the most potent compound of the tested panel) is depicted in **Figure 3**, graphs for other NBOMes can be found in **Supplementary Material S4**.

3.5. In silico evaluation of the 25I-NBOMe – MOR interaction

The performance of the IFD method lies in the fact that the flexibility of the protein-ligand complex allows the receptor to adapt to ligands of different shapes and structures, while also enabling the use of membranes and implicit solvents. Thus, the IFD protocol was used to identify the interactions of 25I-NBOMe, 25I-NBOMe (3-MeO isomer) and 25I-NBOMe (4-MeO isomer) with MOR and to select the poses with the best docking score. IFD results were successively screened by means of an MM-GBSA algorithm to select the poses with the best free-binding energy values. Interestingly, calculations identified two energetically favorable poses for 25I-NBOMe, thereby suggesting two possible different orientations of the ligand inside the receptor (**Table 4**).

In more detail, the more energetically favored 25I-NBOMe (Pose 1) was oriented with the halogenated ring directed towards the outer part of the receptor and the N-methoxybenzyl to the inner one. Pose 2 showed an opposite orientation within MOR. Regarding the considerable receptor hydrophobic surface**, Figure S5.1 (Supplementary Material S5)** shows that both poses were deeply involved in a series of van der Waals interactions, particularly with the aromatic rings and the inner and outer part of MOR. Conversely, the aliphatic chain in between both aromatic rings of the 25I-NBOMe chemical structure appeared poorly involved in receptor interactions.

Noteworthy, though differently oriented within the receptor binding site, both poses showed the key salt bridge contact with the amino acid Asp 147, as already observed for many MOR ligands[36,43,55], and a π-cation contact with Tyr 148. 25I-NBOMe (Pose 1) also showed an additional contact with the inner part of the receptor, due to a $\pi-\pi$ stacking between the methoxyphenyl ring and Tyr 326, while Pose 2 displayed a halogen bond between the iodine substituent and Ile 322 **(Figure 4, panels A & B).** As shown in **Panel C and D in Figure 4**, both isomers displayed the crucial electrostatic contact with Asp 147, but only for 25I-NBOMe (4-MeO isomer) the $\pi-\pi$ stacking between the methoxyphenyl ring and Tyr 326 was evidenced. For comparison, **Panel E** shows the opioid agonist BU 72 involved in interactions with Asp 147 and Tyr 148.

MM-GBSA experiments carried out on both positional isomers of 25I-NBOMe (3-MeO and 4-OMe isomers) evidenced one energetically favorable pose for each ligand. Interestingly, 25I-NBOMe (Pose 1), 25I-NBOMe (4-MeO isomer) and 25I-NBOMe (3-MeO isomer) appeared similarly oriented inside the receptor, with the halogenated ring directed towards the outer part of the receptor and the methoxy phenyl to the inner one **(Figure 5, Panel A)**.

As regards the MOR activation process, we observed that only 25I-NBOMe and 25I-NBOMe (4-MeO isomer) induced some aminoacidic rearrangements at the receptor binding pocket similar to the crystallographic agonist BU72. In particular, both ligands were responsible for a Met 151 flip, which

might be significant in the receptor activation(De Luca et al. 2022). Moreover, a favorable shift of the Ile 155 residue, as well as a rotamer conformational change of Trp 293, could be observed **(Figure 5, Panel B)**.

Interestingly, we also noticed that the less active 25I-NBOMe (3-MeO isomer) displayed an unfavorable steric interaction(Ramachandran et al. 1963) particularly between the iodine atom and His 54 and Ser 53, thus inducing a thermodynamically unlikely occurring receptor conformation. A visual representation of this can be found in **Supplementary Material S5, Figure S5.2**.

4. Discussion

Inspired by the observations by Åstrand et al.(Åstrand et al. 2020), this study aimed at further investigating the in vitro off-target activation potential of several psychedelics at MOR, using a βarr2 recruitment (NanoBiT® MOR-βarr2) and a Ca^{2+} release (AequoScreen®) assay. Additionally, concentration-dependence and specificity of the observed effects were investigated and antagonist experiments as well as molecular docking were performed to substantiate the findings.

4.1. Screening of psychedelics for MOR activity

An extensive set of psychedelics was screened using the MOR-βarr2 assay, including certain substances also analyzed earlier by Åstrand et al., as well as some analogs. The panel was selected to encompass a wide structural diversity, which allowed us to potentially specify this selection of compounds at a later stage. The βarr2 recruitment assay was selected for this purpose, as initial scouting experiments had revealed that the AequoScreen® Ca^{2+} is more susceptible to picking up aspecific effects (vide infra). At a concentration of 25 µM, only five of the evaluated compounds yielded MOR activation. Interestingly, 2C-I, βκ-2C-B, DMT, 5-MeO-DET, 5-IT, Bromo-DragonFLY and TFMPP, all of which were scored by Åstrand et al. to have some opioid activity using an AequoScreen® assay at a concentration of 7.5 µg/mL (same order of magnitude as 25 µM), were found to be inactive at MOR using the MOR-βarr2 assay. While looking into the reason for this apparent discrepancy was not within the scope of this manuscript, the known promiscuous receptor activating potential of several of these compounds (e.g. binding and activating a multitude of 5-HT_2Rs(Porter et al. 1999; Ray 2010; Halberstadt and Geyer 2011; Eshleman et al. 2014, 2018)), combined with a more downstream event being scored by the Aequoscreen® assay (as opposed to a receptor-proximal event scored by the βarr2 assay), may be an obvious explanation.

Out of the 23 psychedelics analyzed in this initial screening, only substances of the NBOMe class (25I-, 25B-, 25C-, 25D- and 25E-NBOMe) demonstrated activity at MOR using the MOR-βarr2 assay. This confirms the findings reported by Åstrand et al., who showed that 25I-NBOMe and 25E-NBOMe could

activate MOR in the AequoScreen® assay, albeit with low potency. These all carry the typical N-benzyl phenethylamine scaffold, substituted at position 4 of the phenethylamine ring structure, with, in this case, respectively a iodo, bromo, chloro, methyl or ethyl group. Interestingly, using a comparable βarr2 recruitment assay at the 5-HT_{2A}R (the prime target of these compounds), Pottie et al. observed that compounds with the NBOMe structure were consistently more potent and efficacious than their phenethylamine counterparts (2C-I, 2C-B, 2C-C, 2C-D, 2C-E)(Pottie et al. 2020a), the latter all being inactive at MOR at a concentration of 25 µM (**Table 1**). In line with this, the unsubstituted 25H-NBOMe, which is about 5- to 10-fold less potent at the 5-HT_{2A}R compared to its substituted analogs(Pottie et al. 2020a, b), was also not capable of activating MOR. Based on this initial screening, our findings at MOR can be considered to display a trend similar to that observed for the activity of these compounds at the target 5-HT_{2A}R, with highly potent NBOMes showing off-target activation of MOR. These observations led to the selection of a panel of 19 new compounds to be screened for MOR activation potential, taking along a number of substances with the NBOMe core structure and a variety of functional groups. By doing this, the potential positive effect on MOR activity of certain structural modifications on the N-benzyl phenethylamine scaffold could be explored.

When tested at a concentration of 25 µM, five compounds from this new, expanded panel were identified as potential MOR agonists: 25iP-NBOMe, 25I-NBOMe (4-methoxy isomer), 25I-NBOH, 25B-NBOH and 25E-NBOH.

Of the additional NBOMes with an alkyl side chain that were analyzed, only the isopropyl-substituted 25iP-NBOMe, but not the n-propyl analog 25P-NBOMe or 25G-NBOMe carrying methyl substituents on position 3 and 4 of the phenyl moiety, showed activity. Also analogs bearing a thioether group (25T-, 25T2- 25T4- and 25T7-NBOMe) or a nitro group (25N-NBOMe) failed to activate MOR, despite some of these compounds being quite potent at 5-HT_{2A}R(Rickli et al. 2015).

Carrying a structural modification at the N-benzyl moiety, 25I-NBF, 25B-NBF and 25I-NBMD were not able to activate MOR. Compounds carrying the NBF or NBMD structural entities were previously also

observed to be less potent and efficacious at 5-HT$_{2A}$R than those containing an NBOMe backbone (Braden et al. 2006; Hansen et al. 2014; Jensen et al. 2017; Pottie et al. 2020a). Furthermore, of the two additional positional isomers of 25I-NBOMe included in our test panel, only the 4-MeO isomer showed MOR activation potential. Neither the imine nor the N-acetyl analog of 25I-NBOMe showed MOR activation potential.

Last, four NBOH analogs were included in this additional panel, only differing from their NBOMe counterparts in the presence of a hydroxyl group - as opposed to a methoxy group - at position 2 of the N-benzyl ring. Looking at 5-HT$_{2A}$R activity, it has been reported that NBOH analogs have a similar activity profile as their NBOMe counterparts(Jensen et al. 2017; Pottie et al. 2020a). Here, all but one of the evaluated NBOH analogs displayed MOR activation potential - only the chlorinated analog (25C-NBOH) failed to activate MOR, as opposed to its 25C-NBOMe analog, which did activate MOR. This is somewhat surprising, as 25C-NBOH is a highly potent 5-HT$_{2A}$R agonist (sub-nM EC_{50}) and suggests that there is no direct 1:1 link between the receptor activation potential of these compounds at the target 5-HT$_{2A}$R, and their potential to result in off-target activation of MOR(Pottie et al. 2020a).

4.2. Pharmacological characterization

Further characterization of the above-described compounds using the MOR-βarr2 recruitment assay revealed that 25I-NBOMe had the highest potency and efficacy of the analyzed set. Based on the concentration-response curves (**Figure 2, Panel A**), 4-methoxy 25I-NBOMe, a positional isomer carrying the methoxy group on position 4 as opposed to position 2, appeared to have a lower potency at MOR. Taking into account the results of the initial screening, which also included the 3-methoxy analog, this demonstrates that for MOR activity, the methoxy group on the N-benzyl structure is preferably on position 2 (25I-NBOMe). The MOR activation potential substantially decreased when moving the substituent to position 4 and position 3, the latter having no activity at MOR. Similarly, using a Ca^{2+} mobilization assay, Nichols et al. reported a decrease in 5-HT$_{2A}$R activity for both 4- and 3-methoxy isomers compared to 25I-NBOMe and a decrease in activity in producing head twitch

response in mice, with the 4-methoxy isomer being inactive here(Nichols et al. 2015). Also, in the AequoScreen® assay, these analogs displayed the same rank order in potencies, with 25I-NBOMe being the most potent compound of the evaluated set **(Figure 2, Panel B)**.

The impact of different halogen substitutions was evaluated by comparing analogs with a iodo (25I-NBOMe), a bromo (25B-NBOMe) and a chloro (25C-NBOMe) group, as depicted in **Figure 2, Panel C, D**. At the 5-HT_{2A}R, the identity of this substituent did not have a profound impact on the activity profile, as demonstrated by the closely overlapping concentration-response curves and very similar EC_{50} values for 25I-, 25B- and 25C-NBOMe(Pottie et al. 2020a). At MOR, the MOR-βarr2 data indicated an increase in potency with increasing size of the halogen atom (I > B > C), which was confirmed using the AequoScreen® assay. Earlier, Rickli et al. observed this trend in 5-HT_{2A}R activation potential for 2C-X compounds, lacking the N-benzyl moiety, but similar to Pottie et al., they did not observe this for the NBOMe analogs(Rickli et al. 2015; Pottie et al. 2020a).

Compared to their NBOMe counterparts, the NBOH analogs demonstrated a clear decrease in activity in both assays. For instance, 25I-NBOH (**Figure 2, Panel A**) had an approximately 10-fold reduced potency, along with a 1.5-fold decrease in efficacy, based on MOR-βarr2 data. For 25E-NBOH, the hydroxyl analog of the ethylated 25E-NBOMe (vide infra), also a decrease in activity could be observed in both assays, albeit less pronounced (**Figure 2, Panel E, F**). MOR-βarr2 data show a similar activity profile for both analogs, with 25E-NBOH being slightly less potent. Interestingly, concentration-response curves for the AequoScreen® assay showed that all NBOH analogs, having a hydroxyl instead of a methoxy substituent on the N-benzyl moiety, behaved as partial agonists, as opposed to their NBOMe counterparts which were full agonists in this assay. This demonstrates that switching the 2-methoxy group to a hydroxyl group is tolerated, but results in a decreased activity. This is not necessarily the case for all NBOH analogs, as 25B-NBOH had almost no activity in the NanoBiT® assay, despite being scored as a partial agonist in the AequoScreen® assay (**Figure 2, Panel G, H**) and 25C-NBOH showed no activity during screening (25µM). Interestingly, the pattern observed earlier for

halogenated NBOMes also appears to be applicable here, as the activity of the NBOH analogs also increased with an increasing size of the halogen atom substituent.

Lastly, focusing on structural analogs carrying an aliphatic side chain, both assays showed an increase in MOR activity with increasing length of the alkyl tail, with the ethyl-substituted 25E-NBOMe being more potent than the methyl-substituted analog 25D-NBOMe (**Figure 2, Panel I, J**). This pattern could not be extrapolated to even longer substituents, as the n-propyl analog failed to activate MOR during the initial screening phase. Interestingly, Rickli et al. reported on the slight decrease in 5-HT$_{2A}$R activity with the size of the alkyl substituent, with 25D-NBOMe being more potent then 25E-NBOMe(Rickli et al. 2015), whereas Pottie et al. observed almost no difference in activity between both analogs(Pottie et al. 2020a). Based on our observations, in order to activate MOR, a small alkyl tail seems preferred for alkyl-NBOMe analogs, with longer or more bulky alkyl chains resulting in a loss of activity, which has also been observed for other psychedelics at 5-HT$_{2A}$R(Nichols et al. 1977; Nichols 2012). In line with this, 25H-NBOMe did not show MOR activation potential during initial screening and, compared to 25E-NBOMe, the isopropyl analog 25iP-NBOMe showed an important decrease in activity in the MOR-βarr2 recruitment assay. Surprisingly, the latter was not observed in the AequoScreen® assay, which revealed a substantial yet unexpected increase in both potency and efficacy for 25iP-NBOMe. To investigate the cause of this deviating activity profile, all analogs were further tested for non-MOR mediated effects, using cells expressing CB_1 (vide infra, section 4.3.).

Looking into the results, it is clear that both assays applied in this study are capable of monitoring MOR activation, albeit at a different level. Measuring both βarr2 recruitment and G protein-mediated intracellular calcium flux, the latter being an event much more downstream the receptor signaling pathway, provides a more comprehensive insight in the behavior of these NBOMes at MOR. Comparing the activation profiles obtained using the NanoBiT® and AequoScreen® assays, some general features can be observed. As mentioned above, although higher potencies were found using the AequoSceen® assay, the same overall trend regarding activity was conserved in both assays – apart from some

exceptions, which can be explained by non-MOR mediated effects in the Aequoscreen® assay (see further, section 4.3.). However, the concentration-response curves look quite distinct, with MOR-βarr2 data showing a broader range of efficacies, whereas graphs for the AequoScreen® data appear to converge towards 100%. Interestingly, all NBOMes and NBOMe analogs acted as partial MOR agonists in the NanoBiT® βarr2 assays, whereas several substances did yield 100% MOR activation in the AequoScreen® assay (relative to reference compound hydromorphone). This discrepancy, as well as assay-specific differences (vide infra) complicate the assessment and comparison of the efficacy values over the different assays. Hence, these particular compounds behave differently from other opioids in the comparative evaluation of these assays, as Vandeputte et al. previously observed for new synthetic opioids that partial agonists identified using the NanoBiT® system were also partial agonists in the AequoScreen® assay(Vandeputte et al. 2022b). Earlier NanoBiT® data also shows that the assay is capable of showing maximal receptor activation way beyond 100% compared to hydromorphone, as demonstrated by activity data for e.g. etonitazene (E_{max} = 316%)(Vandeputte et al. 2022a). Efficacies obtained using the AequoScreen® assay on the other hand, hardly ever exceed 100% due to an effect which is often being referred to as the assay's 'ceiling'. This phenomenon may be explained by a rapid depletion of the biosensor. In short, low calcium concentrations are required for the regeneration of the aequorin protein, however after receptor stimulation, a rapid influx of calcium ions occurs, leaving the aequorin irreversibly bound during the assay(Charlton and Vauquelin 2010). Furthermore, as the assay monitors a more downstream event after receptor activation, there is an important signal amplification, leading to a large increase in intracellular calcium, contributing to a quick saturation of the system(Charlton and Vauquelin 2010). In contrast, βarr2 recruitment assays monitor an event much more proximal to the receptor, and are therefore less subject to signal amplification(Wouters et al. 2019; Gillis et al. 2020). Combined, these differences in assay set-up may explain the distinct activation profiles and why comparison of the observed SAR, based on the potencies obtained using both assays, is more relevant than a side-by-side comparison of efficacy values.

4.3. Determination of non-MOR specific effects

The surprisingly high apparent efficacy of 25iP-NBOMe in the Aequoscreen® assay, combined with the fact that this is a 'downstream' assay, led us to investigate whether interaction with other (non-MOR) targets might be responsible for (part of) the Ca^{2+} mobilization. We therefore submitted all compounds to both a NanoBiT® (βarr2 recruitment-based) and an AequoScreen® CB_1 assay, both highly similar to the used MOR assays, but with the expressed receptor of interest being irrelevant. Whereas none of the compounds induced βarr2 recruitment to CB_1, increased signals in the AequoScreen® CB_1 assay were observed for almost all analogs to varying degrees (**Supplementary Material S3**). This indicates that for these compounds the effects observed using the AequoScreen® MOR assay may represent a combination of both MOR-mediated signaling and one or more MOR-independent events causing intracellular calcium flux. For 25iP-NBOMe, which showed the most prominent non-MOR-mediated effect, these non-specific effects may explain the apparent discrepancy between both assays: this compound yielded the overall highest signals in the AequoScreen® MOR assay (even exceeding the signal of the reference, 128%), although in the MOR-βarr2 recruitment assay its activity was strongly reduced. Similarly, Åstrand et al. also readily suggested that non-receptor-specific effects may take place when using the AequoScreen® assay, as suspected for the phenethylamine-like hallucinogenic substance Bromo-DragonFLY, which showed activity in all four AequoScreen® receptor systems (MOR, CB_1, 5-HT_{2A}, 5-HT_{1A}). The authors hypothesized that this distinct activity profile may be the result of non-specific effects or permeabilization of cell membranes, rather than receptor-mediated signaling(Åstrand et al. 2020). Of note, Bromo-DragonFly did not yield MOR activation in our initial MOR-βarr2-based screening. Further exploration of the exact underlying mechanism for these non-specific effects is beyond the scope of this manuscript. Either way, comparing the outcome of 2 distinct assays has proven beneficial for this study to validate the specificity of MOR activation and to avoid drawing false structure-activity relationship conclusions based on non-MOR mediated effects.

4.4. Orthosteric binding

Given the rather unexpected MOR activation of this distinct class of psychedelics, it remained unclear whether NBOMes bound the common opioid binding pocket, or rather acted as allosteric activators of the receptor. Orthosteric binding was assessed by first blocking MOR with naloxone, a well-established opioid antagonist(Pasternak 2014). Pre-treatment with naloxone was clearly capable of antagonizing MOR activation by NBOMes, even in case of a 25-100-fold molar excess of the latter. This indicates that these substances do bind to the same pocket within MOR as 'conventional' opioids. Moreover, the fact that both βarr2- and G protein-dependent signaling assays were activated indicates that these psychedelics are capable of inducing a similar conformational change of the receptor to modulate downstream signaling pathways.

4.5. In silico evaluation of the 25I-NBOMe – MOR interaction

Subsequently, we decided to evaluate the interaction between the most potent analog 25I-NBOMe, as well as two positional (3-MeO and 4-MeO) isomers, and MOR by means of molecular docking. For 25I-NBOMe, in silico experiments performed on the MOR active form revealed two possible orientations inside MOR, similarly to what was previously observed for fentanyl-MOR binding(Lipiński et al. 2019; Vo et al. 2020; Eshleman et al. 2020; Ricarte et al. 2021; Xie et al. 2022), with Pose 1 (MM-GBSA -113.27 kcal/mol) being the most energetically favorable. Interestingly, compared to the 25I-NBOMe (3-MeO isomer), 25I-NBOMe (Pose 1) and 25I-NBOMe (4-MeO isomer) interacted more deeply with the inner part of the receptor due to the $\pi-\pi$ interaction with Tyr 326. Moreover, in case of the 4-MeO isomer, the absence of the electrostatic contact with Tyr 148 might justify the superior ability of 25I-NBOMe to activate the receptor. These observations match the MOR activation data observed for these compounds, with 25I-NBOMe being more potent than the 4-MeO isomer, and the 3-MeO isomer lacking MOR activation potential. IFD experiments suggested that only 25I-NBOMe and 25I-NBOMe (4-MeO isomer), similarly to the agonist BU72, were able to induce aminoacidic rearrangements that might be crucial during the MOR activation process. Besides, 25I-NBOMe (3-MeO

isomer), although showing good MM-GBSA values, exhibited unfavorable steric interactions with Ser 53 and His 54 that might account for a metastable pose. These findings are in line with the absence of MOR activity of this analog, demonstrated by the initial screening using the MOR βarr2 recruitment assay.

4.6. Relevance and future outlook

The findings presented here contribute to an expanded knowledge on the pharmacological properties of NBOMes and NBOMe analogs, which is often lacking for the rapidly emerging new psychoactive substances. Apart from bioavailability or production of active metabolites, off-target activity may potentially be a contributing factor to the occurrence of toxicity. However, although we showed here MOR activity for these psychedelics, this intrinsic receptor activation potential was rather limited. Furthermore, for most analogs, MOR activation was only observed at a very high (micromolar) concentration. Typically, serum and urine concentrations found in patients hospitalized after NBOMe ingestion were in the ng/mL range, which is several orders of magnitude lower than the highest concentrations analyzed in this study (Rose et al. 2013; Poklis et al. 2014b, a; Suzuki et al. 2015). Hence, we do not anticipate that opioid effects will contribute to NBOMe-associated toxicity, as physiologically relevant concentrations fail to activate MOR. As the off-target activity of these compounds at other receptors is currently largely unexplored, we cannot speculate on the impact or relevance of (other) off-target activity on the experienced toxicity in users. However, we now know that compounds with the N-benzyl phenethylamine structure hold potential for activating MOR. Of particular interest here is that the surge of new substances that continuously enter the NPS market often stems from the introduction of compounds bearing a wide array of functional groups and structural features, which allows them to bypass current legislative control. It is therefore not unlikely that the future synthesis of compounds carrying the common NBOMe structure with a combination of specific structural modifications may yield substances with more pronounced activity at MOR. This may complicate an already very diverse and complex recreational drug market, with substances

potentially even having a dual (MOR/5-HT $_{2A}$R) activity and an unpredictable risk profile. The findings described in this study may be of value for several instances. They may inform drug law enforcement agencies on which types of substances could appear in the future, and also give a first insight in the expected (pharmacological) properties of newly emerging substances, which can be valuable for healthcare workers.

5. Conclusion

This study reported on the off-target activity of NBOMes, a class of psychedelics carrying the N-benzyl phenethylamine scaffold. NBOMes and NBOMe analogs were found to be capable of weakly activating the μ opioid receptor, the main target of opioid analgesics and NPS. Two distinct cell-based assays were used to confirm their structure-activity relationship at MOR. 25I-NBOMe had the highest potency in both assays. Overall, opioid activity increased with an increasing size of a halogen atom substituent and upon increasing length of the alkyl side chain (up to an ethyl group). Additionally, the methoxy substituent is preferably at position 2 of the N-benzyl moiety, with 4- and particularly 3-methoxy isomers showing a decrease or even complete loss in MOR activation potential. Furthermore, some hydroxyl analogs (NBOH) activate MOR, albeit to a lesser extent than their NBOMe counterparts. Aspecific effects were observed for several NBOMes using the AequoScreen® intracellular calcium assay, indicating the importance of using orthogonal assays, as applied here. Importantly, MOR activation was substantially reduced when the receptor was blocked by naloxone, indicating orthosteric receptor binding by the psychedelics. In silico experiments revealed that 25I-NBOMe engages in multiple receptor binding interactions, similar to those observed for other common opioids. Other positional isomers were involved in less receptor contacts, in line with decreased or absent MOR activation potential. In any case, in silico results were consistent with biological activity data. Taking into account the overall low activity at MOR, it is rather unlikely that these psychedelics, at physiological concentrations observed in recreational users, will significantly contribute to pronounced MOR toxicity. Nevertheless, certain structural modifications can potentially lead to compounds with enhanced MOR activity, which may potentially have a profound impact on the current recreational drug market and the treatment strategies in case of intoxication.

6. Acknowledgements

This research was supported by the Research Foundation Flanders (FWO; grant 1S54521N). We gratefully acknowledge Cayman Chemical and Chiron AS for the gifting of the reference standards. Prof. Maudens and Prof Van Nuijs are acknowledged for kindly providing the analytical standards for 2C-I, 2C-B, 2C-C and 5MeO-DALT. The Swedish-led part of the study received funding from the Eurostars-2 Joint Programme (European Commission, E! 113377 (Eurostars-2), NPS-REFORM) with co-funding from the European Union's Horizon 2020 research and innovation program, Sweden's Innovation Agency (grant number 2019-03566), and the Strategic Research Area in Forensic Sciences (Styrkeområdet i forensiska vetenskaper) at Linköping University (grant number 2021-10). "Dr. Antonio Laus gratefully acknowledges the Drug Policies Department, Presidency of the Council of Ministers (Italy) for the fellowship within the project: "Implementazione dell'identificazione e studio degli effetti delle NPS: Sviluppo di una multicentrica di ricerca per potenziare la base dati dell'Osservatorio Nazionale Tossicodipendenze e del Sistema di Allerta Precoce" (Unit Leader for University of Cagliari Prof. MA De Luca)".

Conflict of interest

The authors declare that they have no conflict of interest.

7. References

Åstrand A, Guerrieri D, Vikingsson S, et al (2020) In vitro characterization of new psychoactive substances at the μ-opioid, CB1, 5HT1A, and 5-HT2A receptors-On-target receptor potency and efficacy, and off-target effects. Forensic Sci Int 317:110553. https://doi.org/10.1016/j.forsciint.2020.110553

Bakayan A, Domingo B, Vaquero CF, et al (2017) Fluorescent Protein–photoprotein Fusions and Their Applications in Calcium Imaging. Photochemistry and Photobiology 93:448–465. https://doi.org/10.1111/php.12682

Braden MR, Parrish JC, Naylor JC, Nichols DE (2006) Molecular Interaction of Serotonin 5-HT2A Receptor Residues Phe339(6.51) and Phe340(6.52) with Superpotent N-Benzyl Phenethylamine Agonists. Mol Pharmacol 70:1956–1964. https://doi.org/10.1124/mol.106.028720

Cannaert A, Franz F, Auwärter V, Stove CP (2017) Activity-based detection of consumption of synthetic cannabinoids in authentic urine samples using a stable cannabinoid reporter system. Anal Chem 89:9527–9536. https://doi.org/10.1021/acs.analchem.7b02552

Cannaert A, Storme J, Franz F, et al (2016) Detection and activity profiling of synthetic cannabinoids and their metabolites with a newly developed bioassay. Anal Chem 88:11476–11485. https://doi.org/10.1021/acs.analchem.6b02600

Cannaert A, Storme J, Hess C, et al (2018a) Activity-Based Detection of Cannabinoids in Serum and Plasma Samples. Clinical Chemistry 64:918–926. https://doi.org/10.1373/clinchem.2017.285361

Cannaert A, Vasudevan L, Friscia M, et al (2018b) Activity-Based Concept to Screen Biological Matrices for Opiates and (Synthetic) Opioids. Clinical Chemistry 64:1221–1229. https://doi.org/10.1373/clinchem.2018.289496

Charlton SJ, Vauquelin G (2010) Elusive equilibrium: the challenge of interpreting receptor pharmacology using calcium assays. British Journal of Pharmacology 161:1250–1265. https://doi.org/10.1111/j.1476-5381.2010.00863.x

Connor M, Christie MJ (1999) Opioid Receptor Signalling Mechanisms. Clinical and Experimental Pharmacology and Physiology 26:493–499. https://doi.org/10.1046/j.1440-1681.1999.03049.x

De Luca MA, Tocco G, Mostallino R, et al (2022) Pharmacological characterization of novel synthetic opioids: Isotonitazene, metonitazene, and piperidylthiambutene as potent μ-opioid receptor agonists. Neuropharmacology 221:109263. https://doi.org/10.1016/j.neuropharm.2022.109263

Deng L, Vysotski ES, Markova SV, et al (2005) All three Ca2+-binding loops of photoproteins bind calcium ions: The crystal structures of calcium-loaded apo-aequorin and apo-obelin. Protein Science 14:663–675. https://doi.org/10.1110/ps.041142905

Dixon AS, Schwinn MK, Hall MP, et al (2016) NanoLuc Complementation Reporter Optimized for Accurate Measurement of Protein Interactions in Cells. ACS Chem Biol 11:400–408. https://doi.org/10.1021/acschembio.5b00753

Domino EF (1986) Opioid-hallucinogen interactions. Pharmacology Biochemistry and Behavior 24:401–405. https://doi.org/10.1016/0091-3057(86)90370-9

Eshleman AJ, Forster MJ, Wolfrum KM, et al (2014) Behavioral and neurochemical pharmacology of six psychoactive substituted phenethylamines: mouse locomotion, rat drug discrimination and in vitro receptor and transporter binding and function. Psychopharmacology 231:875–888. https://doi.org/10.1007/s00213-013-3303-6

Eshleman AJ, Nagarajan S, Wolfrum KM, et al (2020) Affinity, potency, efficacy, selectivity, and molecular modeling of substituted fentanyls at opioid receptors. Biochemical Pharmacology 182:114293. https://doi.org/10.1016/j.bcp.2020.114293

Eshleman AJ, Wolfrum KM, Reed JF, et al (2018) Neurochemical pharmacology of psychoactive substituted N-benzylphenethylamines: High potency agonists at 5-HT2A receptors. Biochemical Pharmacology 158:27–34. https://doi.org/10.1016/j.bcp.2018.09.024

Ettrup A, Hansen M, Santini MA, et al (2011) Radiosynthesis and in vivo evaluation of a series of substituted 11C-phenethylamines as 5-HT2A agonist PET tracers. Eur J Nucl Med Mol Imaging 38:681–693. https://doi.org/10.1007/s00259-010-1686-8

European Monitoring Centre for Drugs and Drug Addiction (2014) Report on the risk assessment of 2-(4-iodo-2,5-dimethoxyphenyl)-N-(2-methoxybenzyl) ethanamine (25I-NBOMe) in the framework of the Council Decision on new psychoactive substances. Luxembourg

European Monitoring Centre for Drugs and Drug Addiction (2022) European Drug Report: Trends and Developments 2022. Publications Office of the European Union, Luxembourg

Gillis A, Kliewer A, Kelly E, et al (2020) Critical Assessment of G Protein-Biased Agonism at the μ-Opioid Receptor. Trends in Pharmacological Sciences 41:947–959. https://doi.org/10.1016/j.tips.2020.09.009

Glennon RA, Titeler M, McKenney JD (1984) Evidence for 5-HT2 involvement in the mechanism of action of hallucinogenic agents. Life Sciences 35:2505–2511. https://doi.org/10.1016/0024-3205(84)90436-3

Greenwood JR, Calkins D, Sullivan AP, Shelley JC (2010) Towards the comprehensive, rapid, and accurate prediction of the favorable tautomeric states of drug-like molecules in aqueous solution. J Comput Aided Mol Des 24:591–604. https://doi.org/10.1007/s10822-010-9349-1

Halberstadt AL, Geyer MA (2011) Multiple receptors contribute to the behavioral effects of indoleamine hallucinogens. Neuropharmacology 61:364–381. https://doi.org/10.1016/j.neuropharm.2011.01.017

Hansen M, Phonekeo K, Paine JS, et al (2014) Synthesis and Structure–Activity Relationships of N-Benzyl Phenethylamines as 5-HT2A/2C Agonists. ACS Chem Neurosci 5:243–249. https://doi.org/10.1021/cn400216u

Harder E, Damm W, Maple J, et al (2016) OPLS3: A Force Field Providing Broad Coverage of Drug-like Small Molecules and Proteins. J Chem Theory Comput 12:281–296. https://doi.org/10.1021/acs.jctc.5b00864

Huang W, Manglik A, Venkatakrishnan AJ, et al (2015) Structural insights into μ-opioid receptor activation. Nature 524:315–321. https://doi.org/10.1038/nature14886

Jensen AA, McCorvy JD, Leth-Petersen S, et al (2017) Detailed Characterization of the In Vitro Pharmacological and Pharmacokinetic Properties of N-(2-Hydroxybenzyl)-2,5-Dimethoxy-4-Cyanophenylethylamine (25CN-NBOH), a Highly Selective and Brain-Penetrant 5-HT2A Receptor Agonist. J Pharmacol Exp Ther 361:441–453. https://doi.org/10.1124/jpet.117.239905

Johnson MW, Hendricks PS, Barrett FS, Griffiths RR (2019) Classic psychedelics: An integrative review of epidemiology, therapeutics, mystical experience, and brain network function. Pharmacology & Therapeutics 197:83–102. https://doi.org/10.1016/j.pharmthera.2018.11.010

Keiser MJ, Setola V, Irwin JJ, et al (2009) Predicting new molecular targets for known drugs. Nature 462:175–181. https://doi.org/10.1038/nature08506

Kyriakou C, Marinelli E, Frati P, et al (2015) NBOMe: new potent hallucinogens – pharmacology, analytical methods, toxicities, fatalities: a review. European Review for Medical and Pharmacological Sciences 19:3270–3281

Lipiński PFJ, Jarończyk M, Dobrowolski JCz, Sadlej J (2019) Molecular dynamics of fentanyl bound to μ-opioid receptor. J Mol Model 25:144. https://doi.org/10.1007/s00894-019-3999-2

Luethi D, Liechti ME (2020) Designer drugs: mechanism of action and adverse effects. Arch Toxicol 94:1085–1133. https://doi.org/10.1007/s00204-020-02693-7

Madhavi Sastry G, Adzhigirey M, Day T, et al (2013) Protein and ligand preparation: parameters, protocols, and influence on virtual screening enrichments. J Comput Aided Mol Des 27:221–234. https://doi.org/10.1007/s10822-013-9644-8

Manglik A, Kruse AC, Kobilka TS, et al (2012) Crystal structure of the μ-opioid receptor bound to a morphinan antagonist. Nature 485:321–326. https://doi.org/10.1038/nature10954

Marek GJ (2003) Behavioral evidence for μ-opioid and 5-HT2A receptor interactions. European Journal of Pharmacology 474:77–83. https://doi.org/10.1016/S0014-2999(03)01971-X

Nichols DE (2016) Psychedelics. Pharmacol Rev 68:264–355. https://doi.org/10.1124/pr.115.011478

Nichols DE (2004) Hallucinogens. Pharmacology & Therapeutics 101:131–181. https://doi.org/10.1016/j.pharmthera.2003.11.002

Nichols DE (2012) Structure–activity relationships of serotonin 5-HT2A agonists. Wiley Interdisciplinary Reviews: Membrane Transport and Signaling 1:559–579. https://doi.org/10.1002/wmts.42

Nichols DE, Frescas SP, Chemel BR, et al (2008) High Specific Activity Tritium-Labeled N-(2-methoxybenzyl)-2,5-dimethoxy-4-iodophenethylamine (INBMeO): A High Affinity 5-HT2A Receptor-Selective Agonist Radioligand. Bioorg Med Chem 16:6116–6123. https://doi.org/10.1016/j.bmc.2008.04.050

Nichols DE, Sassano MF, Halberstadt AL, et al (2015) N-Benzyl-5-methoxytryptamines as Potent Serotonin 5-HT2 Receptor Family Agonists and Comparison with a Series of Phenethylamine Analogues. ACS Chem Neurosci 6:1165–1175. https://doi.org/10.1021/cn500292d

Nichols DE, Shulgin AT, Dyer DC (1977) Directional lipophilic character in a series of psychotomimetic phenethylamine derivatives. Life Sciences 21:569–576. https://doi.org/10.1016/0024-3205(77)90099-6

Niedernberg A, Tunaru S, Blaukat A, et al (2003) Comparative Analysis of Functional Assays for Characterization of Agonist Ligands at G Protein–Coupled Receptors. SLAS Discovery 8:500–510. https://doi.org/10.1177/1087057103257555

Pasternak GW (2014) Opiate Pharmacology and Relief of Pain. J Clin Oncol 32:1655–1661. https://doi.org/10.1200/JCO.2013.53.1079

Poklis JL, Devers KG, Arbefeville EF, et al (2014a) Postmortem detection of 25I-NBOMe [2-(4-iodo-2,5-dimethoxyphenyl)-N-[(2-methoxyphenyl)methyl]ethanamine] in fluids and tissues determined by high performance liquid chromatography with tandem mass spectrometry from a traumatic death. Forensic Science International 234:e14–e20. https://doi.org/10.1016/j.forsciint.2013.10.015

Poklis JL, Nanco CR, Troendle MM, et al (2014b) Determination of 4-bromo-2,5-dimethoxy-N-[(2-methoxyphenyl)methyl]-benzeneethanamine (25B-NBOMe) in serum and urine by high performance liquid chromatography with tandem mass spectrometry in a case of severe intoxication. Drug Testing and Analysis 6:764–769. https://doi.org/10.1002/dta.1522

Porter RHP, Benwell KR, Lamb H, et al (1999) Functional characterization of agonists at recombinant human 5-HT2A, 5-HT2B and 5-HT2C receptors in CHO-K1 cells. British Journal of Pharmacology 128:13–20. https://doi.org/10.1038/sj.bjp.0702751

Pottie E, Cannaert A, Stove CP (2020a) In vitro structure–activity relationship determination of 30 psychedelic new psychoactive substances by means of β-arrestin 2 recruitment to the serotonin 2A receptor. Arch Toxicol 94:3449–3460. https://doi.org/10.1007/s00204-020-02836-w

Pottie E, Dedecker P, Stove CP (2020b) Identification of psychedelic new psychoactive substances (NPS) showing biased agonism at the 5-HT2AR through simultaneous use of β-arrestin 2 and miniGαq bioassays. Biochem Pharmacol 182:114251. https://doi.org/10.1016/j.bcp.2020.114251

Poulie CBM, Jensen AA, Halberstadt AL, Kristensen JL (2020) DARK Classics in Chemical Neuroscience: NBOMes. ACS Chem Neurosci 11:3860–3869. https://doi.org/10.1021/acschemneuro.9b00528

Ramachandran GN, Ramakrishnan C, Sasisekharan V (1963) Stereochemistry of polypeptide chain configurations. Journal of Molecular Biology 7:95–99. https://doi.org/10.1016/S0022-2836(63)80023-6

Ray TS (2010) Psychedelics and the Human Receptorome. PLOS ONE 5:e9019. https://doi.org/10.1371/journal.pone.0009019

Ricarte A, Dalton JAR, Giraldo J (2021) Structural Assessment of Agonist Efficacy in the μ-Opioid Receptor: Morphine and Fentanyl Elicit Different Activation Patterns. J Chem Inf Model 61:1251–1274. https://doi.org/10.1021/acs.jcim.0c00890

Rickli A, Luethi D, Reinisch J, et al (2015) Receptor interaction profiles of novel N-2-methoxybenzyl (NBOMe) derivatives of 2,5-dimethoxy-substituted phenethylamines (2C drugs). Neuropharmacology 99:546–553. https://doi.org/10.1016/j.neuropharm.2015.08.034

Rose SR, Poklis JL, Poklis A (2013) A case of 25I-NBOMe (25-I) intoxication: a new potent 5-HT2A agonist designer drug. Clinical Toxicology 51:174–177. https://doi.org/10.3109/15563650.2013.772191

Scotton WJ, Hill LJ, Williams AC, Barnes NM (2019) Serotonin Syndrome: Pathophysiology, Clinical Features, Management, and Potential Future Directions. Int J Tryptophan Res 12:1178646919873925. https://doi.org/10.1177/1178646919873925

Sherman W, Day T, Jacobson MP, et al (2006) Novel Procedure for Modeling Ligand/Receptor Induced Fit Effects. J Med Chem 49:534–553. https://doi.org/10.1021/jm050540c

Shimomura O, Johnson FH, Morise H (1974) Mechanism of the luminescent intramolecular reaction of aequorin. Biochemistry 13:3278–3286. https://doi.org/10.1021/bi00713a016

Stables J, Green A, Marshall F, et al (1997) A Bioluminescent Assay for Agonist Activity at Potentially Any G-Protein-Coupled Receptor. Analytical Biochemistry 252:115–126. https://doi.org/10.1006/abio.1997.2308

Suzuki J, Dekker MA, Valenti ES, et al (2015) Toxicities Associated With NBOMe Ingestion—A Novel Class of Potent Hallucinogens: A Review of the Literature. Psychosomatics 56:129–139. https://doi.org/10.1016/j.psym.2014.11.002

United Nations Office on Drugs and Crime (2021) Current NPS Threats. Vienna

United Nations Office on Drugs and Crime (2020) Current NPS Threats. Vienna

United Nations Office on Drugs and Crime (2022) World Drug Report 2022. Vienna

Vandeputte MM, Cannaert A, Stove CP (2020) In vitro functional characterization of a panel of non-fentanyl opioid new psychoactive substances. Arch Toxicol 94:3819–3830. https://doi.org/10.1007/s00204-020-02855-7

Vandeputte MM, Krotulski AJ, Walther D, et al (2022a) Pharmacological evaluation and forensic case series of N-pyrrolidino etonitazene (etonitazepyne), a newly emerging 2-benzylbenzimidazole 'nitazene' synthetic opioid. Arch Toxicol 96:1845–1863. https://doi.org/10.1007/s00204-022-03276-4

Vandeputte MM, Persson M, Walther D, et al (2022b) Characterization of recent non-fentanyl synthetic opioids via three different in vitro μ-opioid receptor activation assays. Arch Toxicol 96:877–897. https://doi.org/10.1007/s00204-021-03207-9

Vasudevan L, Vandeputte M, Deventer M, et al (2020) Assessment of structure-activity relationships and biased agonism at the Mu opioid receptor of novel synthetic opioids using a novel, stable bio-assay platform. Biochemical Pharmacology 177:113910. https://doi.org/10.1016/j.bcp.2020.113910

Vo QN, Mahinthichaichan P, Shen J, Ellis CR (2021) How μ-opioid receptor recognizes fentanyl. Nat Commun 12:984. https://doi.org/10.1038/s41467-021-21262-9

Vo QN, Mahinthichaichan P, Shen J, Ellis CR (2020) How μ-Opioid Receptor Recognizes Fentanyl. bioRxiv 2020.08.16.253013. https://doi.org/10.1101/2020.08.16.253013

Vysotski ES, Lee J (2004) Ca2+-Regulated Photoproteins: Structural Insight into the Bioluminescence Mechanism. Acc Chem Res 37:405–415. https://doi.org/10.1021/ar0400037

Wouters E, Walraed J, Banister SD, Stove CP (2019) Insights into biased signaling at cannabinoid receptors: synthetic cannabinoid receptor agonists. Biochemical Pharmacology 169:113623. https://doi.org/10.1016/j.bcp.2019.08.025

Xie B, Goldberg A, Shi L (2022) A comprehensive evaluation of the potential binding poses of fentanyl and its analogs at the μ-opioid receptor. Comput Struct Biotechnol J 20:2309–2321. https://doi.org/10.1016/j.csbj.2022.05.013

Table 1: Screening of a set of psychedelics at a concentration of 25 µM for activity at the µ opioid receptor, using the NanoBiT® assay. Substances in bold were previously reported by Åstrand et al.(Åstrand et al. 2020) to have MOR activation potential using the AequoScreen® assay. Of the compounds that were also evaluated there, only 25I- and 25E-NBOMe showed MOR activity in the βarr2 assay, 2C-I, Bromo-DragonFLY, 5-IT, βK-C-B, DMT, 5-MeO-DET and TFMPP did not yield a positive MOR signal.

MOR activity detected	**No MOR activity detected**			
Phenethylamine analogs	Phenethylamines	Phenethylamine	Tryptamines	Piperazines
25I-NBOMe	**2C-I**	analogs	**DMT**	**TFMPP**
25B-NBOMe	2C-B	**Bromo-DragonFLY**	DPT	
25C-NBOMe	2C-C	2C-B-FLY	DiPT	Ergolines
25D-NBOMe	2C-D	**5-IT**		LSD
25E-NBOMe	2C-E	**βK-2C-B**	**5-MeO-DET**	
	2C-H	25H-NBOMe	5-MeO-DALT	

Table 2: Overview of the expanded NBOMe panel for MOR screening (25 µM) using the NanoBiT® assay, based on the initial findings regarding the MOR activation potential of five NBOMe analogs. Substances indicated in bold activated MOR.

MOR activity detected after initial screening			
25I-NBOMe, 25B-NBOMe, 25C-NBOMe, 25D-NBOMe, 25E-NBOMe			
Expanded NBOMe panel			
Alkyl group	Thioether group	Nitro group	25I-NBOMe positional isomers
25P-NBOMe	25T-NBOMe	25N-NBOMe	25I-NBOMe (3-MeO isomer)
25iP-NBOMe	25T2-NBOMe		**25I-NBOMe (4-MeO isomer)**
25G-NBOMe	25T4-NBOMe		
	25T7-NBOMe		
NBOH analogs	NBF analogs	NBMD analog	25I-NBOMe analogs
25I-NBOH	25I-NBF	25I-NBMD	25I-NBOMe imine
25B-NBOH	25B-NBF		N-acetyl 25I-NBOMe
25C-NBOH			
25E-NBOH			

Table 3: Pharmacological parameters for efficacy (E_{max}, relative to hydromorphone) and potency (EC_{50}) of NBOMe and NBOH analogs at MOR, determined by application of two distinct cell-based assays (NanoBiT® assay and AequoScreen® assay).

Compound	R_1	R_2	R_3	NanoBiT® βarr2 recruitment assay		AequoScreen® Calcium release assay	
				E_{max} (%) * (95% CI)	EC_{50} (μM) (95% CI)	E_{max} (%) * (95% CI)	EC_{50} (μM) (95% CI)
25I-NBOMe	I	OCH_3	H	**22.9** (20.8-25.3)	**2.74** (1.55-5.06)	**97.0** (95.6-98.4)	**0.88** (780-984)
25I-NBOMe (4-MeO isomer)	I	H	OCH_3	7[a]	>400 x 10^3	84[a]	>18
25I-NBOH	I	OH	H	**15.8** (11.7-24.3)	**23.4** (10.9-55.5)	**54.6** (52.6-56.8)	**1.33** (1.00-1.78)
25B-NBOMe	Br	OCH_3	H	8[b]	>22	**93.6** (89.8-96.9)	**4.73** (3.61– 6.10)
25B-NBOH	Br	OH	H	<5[a]	>12	**57.0** (55.0-59.0)	**5.96** (5.10 -6.95)
25E-NBOMe	Ethyl	OCH_3	H	20[a]	>72	103[a]	> 12.4
25E-NBOH	Ethyl	OH	H	19[a]	>270	**58.4** (54.8-62.2)	**3.78** (2.80-5.09)
25iP-NBOMe	Isopropyl	OCH_3	H	6[a]	>1 x 10^3	128[a]	>27
25D-NBOMe	Methyl	OCH_3	H	<5[a]	>842 x 10^3	72[a]	>63
25C-NBOMe	Cl	OCH_3	H	<5[a]	>122	**81.6** (77.3-86.1)	**10.0** (8.08-12.04)
Hydromorphone	**/**			**100** (94.5-106.4)	**34.5 (nM)** (23.8-49.7)	**98.5** (95.4-101.6)	**15.5 (nM)** (12.4-19.5)

Table shows substitutions of the basic N-benzyl phenethylamine structure, as provided in Figure 1.

*E_{max} values relative to the E_{max} of the reference hydromorphone, set at 100%.

[a] Maximal activation seen at 100 μM. Plateau of maximal activation was not reached, therefore estimated EC_{50} values should be interpreted with caution.

[b] Maximal activation seen at 75 μM. Plateau of maximal activation was not reached, therefore estimated EC_{50} values should be interpreted with caution.

Table 4: IFD and MM-GBSA scores for 25I-NBOMe (Pose 1), 25I-NBOMe (Pose 2), 25I-NBOMe (3-OMe isomer) and 25I-NBOMe (4-OMe isomer) and the crystallographic ligand BU72.

COMPOUNDS	IFD EXTENDED SAMPLE (kcal/mol)	MM-GBSA (kcal/mol)
25I-NBOMe (Pose 1)	-11473.76	-113.27
25I-NBOMe (Pose 2)	-11471.18	-100.41
25I-NBOMe (3-MeO isomer)	-11541.37	-105.48
25I-NBOMe (4-MeO isomer)	-11538.49	-104.38
BU 72	-11531.97	-135.72

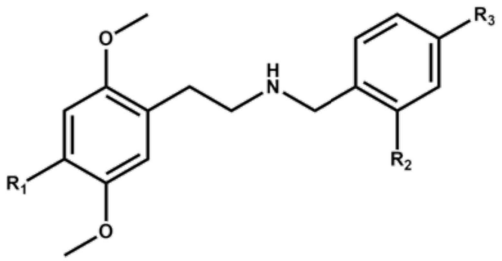

***N*-benzyl phenethylamines**

Figure 1: General N-benzyl phenethylamine structure, present in NBOMes and NBOMe analogs. The R-groups refer to the functional groups indicated in **Table 3**. Chemical structure generated with ChemDraw 19.

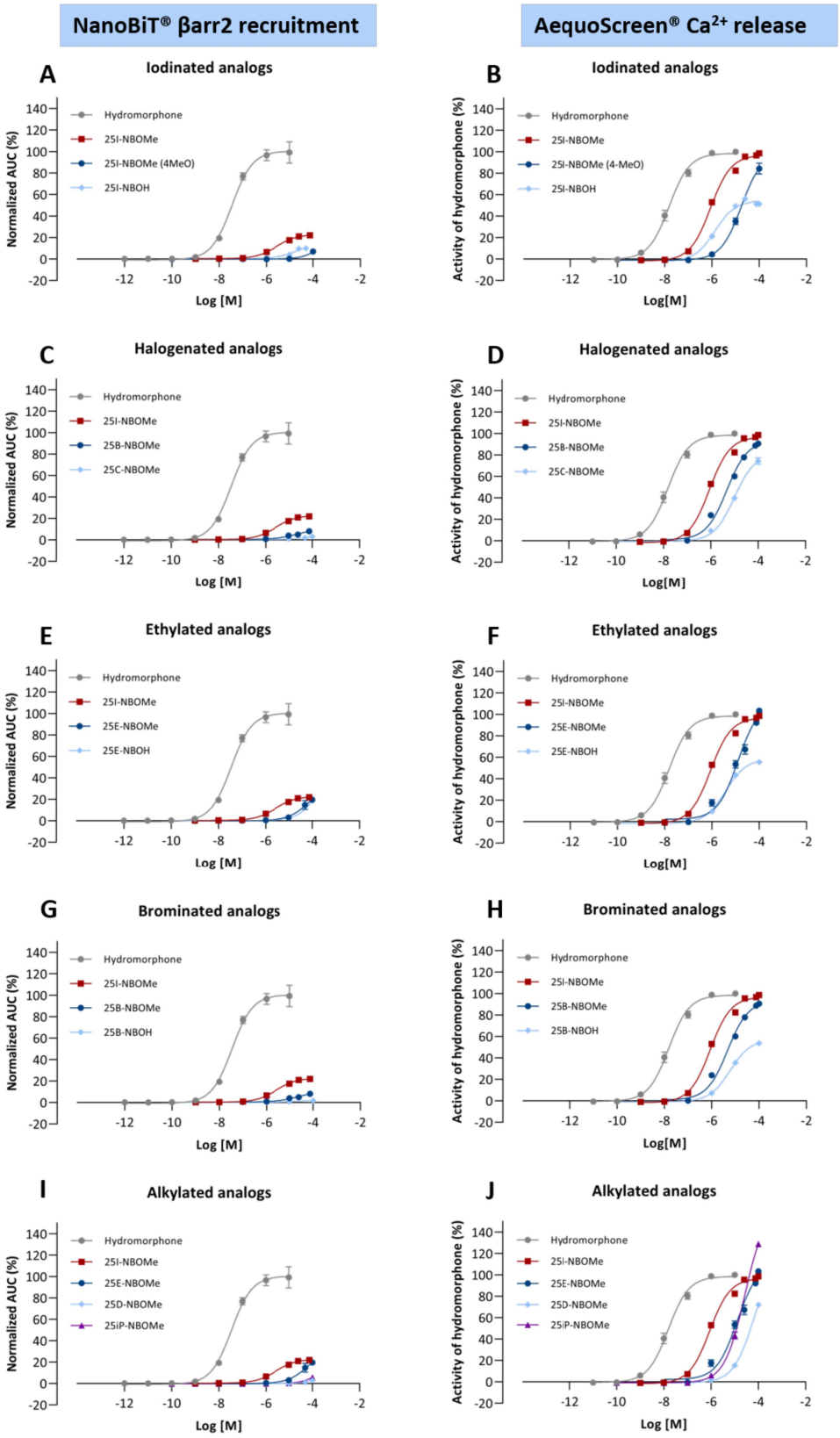

Figure 2: Activation profiles (n ≥ 3) for NBOMe analogs carrying a iodo group (25I-NBOMe, 25I-NBOMe (4-MeO isomer) and 25I-NBOH) (**Panel A and B**), carrying a halogen substituent (25I-NBOMe, 25B-NBOMe and 25C-NBOMe) (**Panel C and D**), carrying an ethyl group (25E-NBOMe and 25E-NBOH) (**Panel E and F**), carrying a bromo group (25B-NBOMe and 25B-NBOH)

(**Panel G and H**), or carrying an aliphatic side chain (25E-NBOMe, 25D-NBOMe and 25iP-NBOMe) (**Panel I and J**). The reference standard hydromorphone and 25I-NBOMe are depicted in each graph. The left and right panels of the figure represent data obtained using the NanoBiT® βarr2 recruitment assay and the AequoScreen® Ca^{2+} release assay, respectively. Data points represent the mean MOR activation ± standard error of the mean (SEM) of at least three independent experiments, with each test condition run in duplicate, all normalized to the E_{max} of hydromorphone.

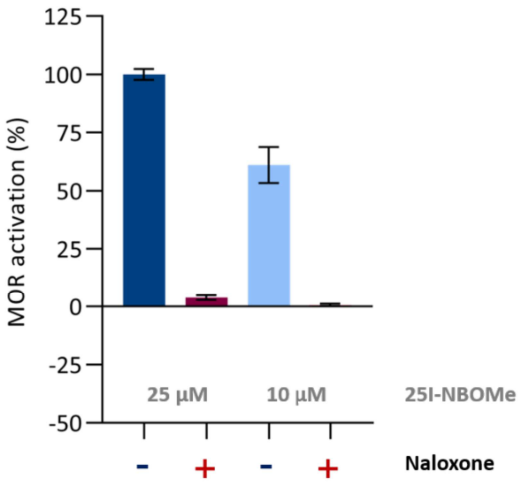

Figure 3: MOR activation by 25 µM and 10 µM 25I-NBOMe, in absence (-, blue) and in presence (+, red) of 1 µM naloxone (n = 3). Data represent the area under the curve (AUC) ± standard error of the mean (SEM), normalized to the AUC of 25 µM of 25I-NBOMe.

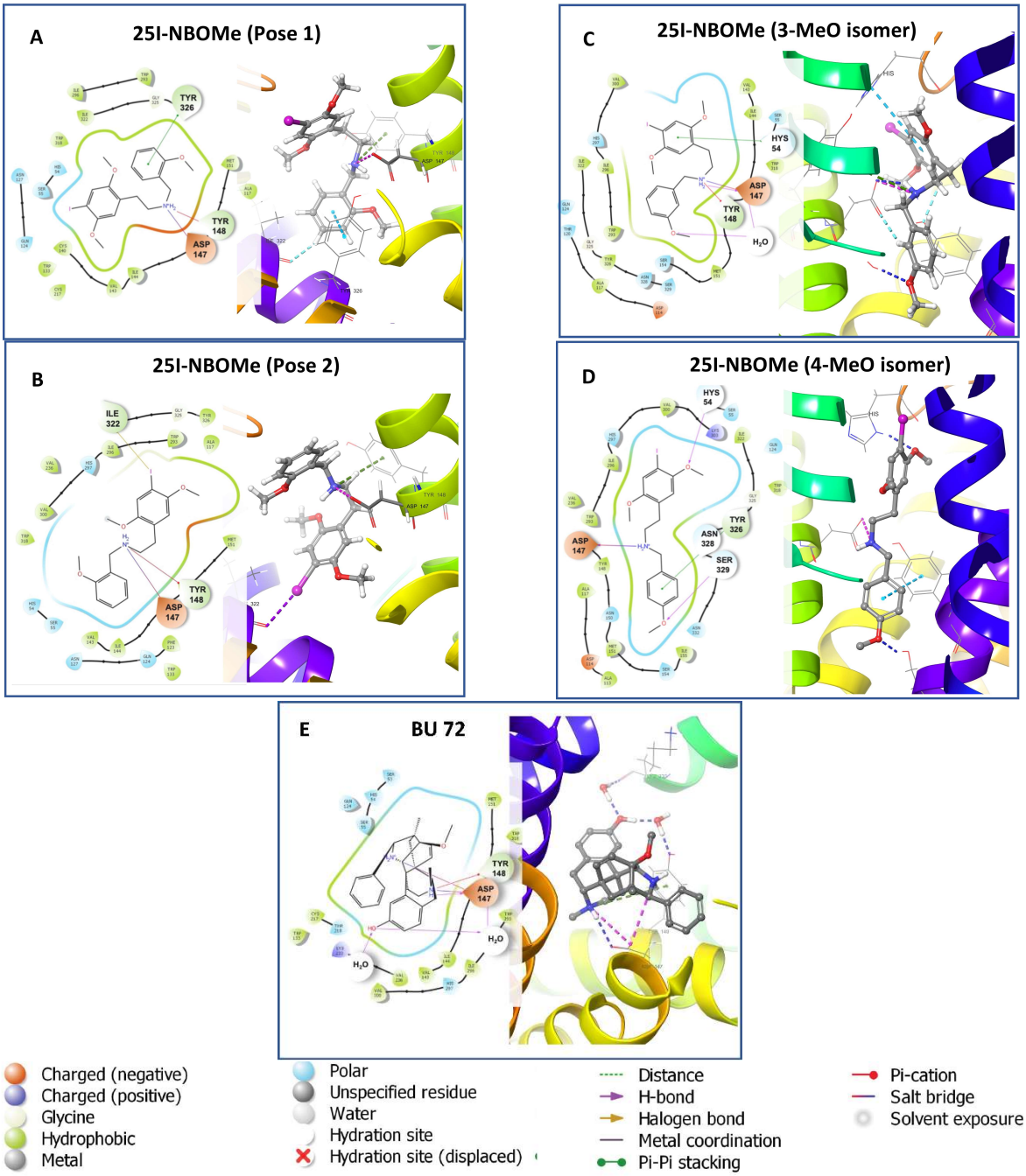

Figure 4: Electrostatic interactions within the μ opioid receptor binding site for (A) 25I-NBOMe (Pose 1), (B) MOR/25I-NBOMe (Pose 2), (C) 25I-NBOMe (3-MeO isomer), (D) 25I-NBOMe (4-MeO isomer) and (E) BU 72.

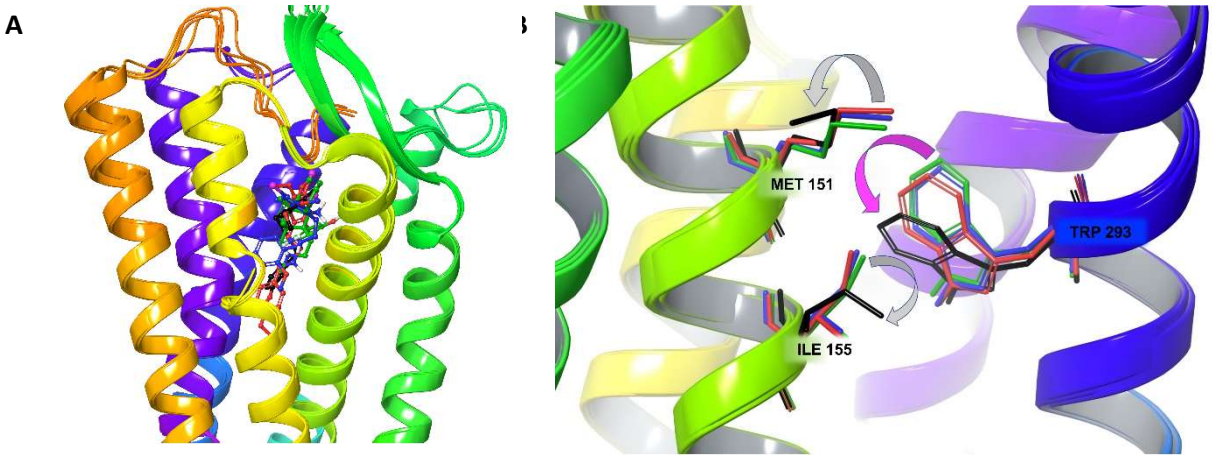

Figure 5: (A) Superimposition of the lowest free binding energy poses of 25I-NBOMe (Pose 1) (blue), 25I-NBOMe (3-MeO isomer) (black), 25I-NBOMe (4-MeO isomer) (red) and BU 72 (green) inside the MOR pocket and (B) structural rearrangements during receptor activation of Met 151 and Ile 155 residues (grey arrows) and rotamer conformational change of Trp 293 (purple arrow), when bound to 25I-NBOMe (Pose 1) (blue), 25I-NBOMe (3-MeO isomer) (black) and 25I-NBOMe (4-MeO isomer) (red) and BU 72 (green).